

# Predictive Model for Macular Hole Closure Speed: Insights From Intraoperative Optical Coherence Tomography

Justis P. Ehlers<sup>1,2</sup>, Atsuro Uchida<sup>1,2</sup>, Sunil K. Srivastava<sup>1,2</sup>, and Ming Hu<sup>1,3</sup>

<sup>1</sup> The Tony and Leona Campane Center for Excellence in Image-Guided Surgery and Advanced Imaging Research, Cole Eye Institute, Cleveland Clinic, Cleveland, OH, USA

<sup>2</sup> Cole Eye Institute, Cleveland Clinic, Cleveland, OH, USA

<sup>3</sup> Department of Quantitative Health Sciences, Lerner Research Institute, Cleveland Clinic, Cleveland, OH, USA

**Correspondence:** Justis P. Ehlers, Cole Eye Institute, Cleveland Clinic, 9500 Euclid Avenue/i32, Cleveland, OH 44195, USA. e-mail: ehlersj@ccf.org

**Received:** 25 June 2018

**Accepted:** 18 November 2018

**Published:** 6 February 2019

**Keywords:** intraoperative optical coherence tomography; macular hole

**Citation:** Ehlers JP, Uchida A, Srivastava SK, Hu M. Predictive model for macular hole closure speed: insights from intraoperative optical coherence tomography. *Trans Vis Sci Tech.* 2019;8(1):18, <https://doi.org/10.1167/tvst.8.1.18>  
Copyright 2019 The Authors

**Purpose:** To establish a predictive model of macular hole (MH) closure speed.

**Methods:** This study was a post hoc analysis of eyes that underwent full-thickness MH repair in the prospective PIONEER intraoperative optical coherence tomography (iOCT) study. The Biotigen SDOIS system was used for iOCT imaging. All patients underwent standard small-gauge vitrectomy with internal limiting membrane (ILM) peeling, gas tamponade, and postoperative facedown positioning. Before vitrectomy and after ILM peeling, various quantitative OCT measures related to MH were obtained, including MH geometry alterations and outer retinal features. Trans-gas OCT was performed on postoperative day 1 to evaluate MH closure. Univariate and multivariate analyses were conducted to identify predictors of early MH closure (i.e., postoperative day 1 [POD 1] closure).

**Results:** Thirty-two (86%) out of 37 eyes were confirmed for MH closure at POD 1. At 3 months, MH closure was achieved in 35 (95%) eyes. After multivariate logistic regression analyses, seven covariates were determined as predictors for MH closure. These seven covariates included age, ellipsoid zone-retinal pigment epithelium expansion following ILM peel, preincision minimal width, post-ILM peel MH depth, change in MH volume, change in minimum MH width, and change in MH depth. Using these seven covariates, the area under the curve was 0.974. Cross-validation analysis indicated that intraoperative change in MH volume, intraoperative change in minimal width, and preincision minimal width were the most robust predictors for early MH.

**Conclusions:** This study suggests that iOCT may be important in predicting MH closure speed and may be a surrogate for tissue properties/behavior. A future prospective clinical trial is needed to validate this model.

**Translational Relevance:** This study provides unique insights into the potential role of iOCT imaging in predicting retinal tissue behavior during MH repair.

## Introduction

Surgical repair and postoperative management for full-thickness macular hole (MH) has evolved significantly since Kelly and Wendel<sup>1</sup> first described the benefit of vitrectomy and gas tamponade in 1991. With the advent of vital dyes and thanks to modifications to the surgical technique, such as internal limiting membrane (ILM) peeling, MH has become a treatable disease with a high anatomical success rate reaching 90% to 95%.<sup>2-4</sup> Despite these improvements, there is

continued debate over whether postoperative posturing or prolonged gas tamponade is necessary.<sup>5-10</sup>

Since the immobility arising from prolonged postoperative facedown positioning negatively impacts a patient's quality of life and causes occasional but severe adverse events,<sup>11-14</sup> there has been an attempt to alleviate patient discomfort by shortening the duration of posturing.<sup>6-10,15-18</sup> Previous studies suggested that smaller holes may require minimal or no facedown positioning.<sup>8,9</sup> Some investigators have utilized postoperative optical coherence tomography (OCT) analysis in gas-filled eyes to confirm early

closure of the MH and to individualize the period of posturing,<sup>7,15–18</sup> they have indicated that around 10% of MHs may still require facedown positioning.<sup>7</sup> Other investigators have focused on utilizing preoperative OCT variables or indices to predict anatomical success.<sup>19–22</sup> However, in the absence of a large prospective trial on facedown positioning, a reliable method for determining the position requirement is still lacking, and no consensus has been reached on actual duration of posturing.<sup>5,6,8–10</sup> Accurate methods for predicting MH closure speed remain unclear. Therefore, many patients are instructed to maintain facedown positioning for a longer period than deemed necessary.

Recently introduced intraoperative OCT (iOCT) has provided a unique opportunity for visualization of surgical manipulations and has identified novel pathologic conditions of various retinal diseases.<sup>23–28</sup> During MH repair, iOCT has demonstrated that ultrastructural details of MH can be appreciated and surgically induced dynamic morphologic alterations of the fovea can be examined and measured intraoperatively.<sup>29–31</sup> Preliminary studies have suggested that many of these dynamic intraoperative variables may play a role in anatomical normalization following surgical repair.<sup>30</sup> The purpose of the present study was to develop a predictive model of MH closure speed with high sensitivity and high specificity, utilizing a panel of biomarkers based on iOCT.

## Methods

The PIONEER (Perioperative Ophthalmic Imaging with Optical Coherence Tomography) study is a single-site, multisurgeon, prospective study investigating the role of iOCT in ophthalmic surgery.<sup>23</sup> The study, which included a standardized imaging protocol utilizing iOCT imaging obtained at various surgical milestones, was approved by the Cleveland Clinic Institutional Review Board and adhered to all the tenets of the Declaration of Helsinki. The overall methods of the procedures have been previously described.<sup>23</sup> Written informed consent was obtained from all patients after a full explanation of the study was given by a study investigator.

Among participants enrolled in the PIONEER study, patients who had a surgical intervention for full-thickness MH were identified. Of those, eyes that underwent ILM peeling were included in this analysis. Intraoperative imaging for this portion of the PIONEER study was performed using a Bioptigen SDOIS system (Bioptigen, Inc., Research Triangle

Park, NC); a noncontact wide-angle viewing system or magnified contact lens was utilized for fundus observation and iOCT visualization. Exclusion criteria included lack of trans-gas OCT image on the first postoperative day (POD 1) and insufficient iOCT quality for quantitative analysis.

## Surgical Procedure

All patients with MH underwent standard three-port 23-gauge or 25-gauge pars plana vitrectomy performed by one of the four retina specialists. For phakic eyes, phacoemulsification and simultaneous intraocular lens (IOL) implantation were performed. After completion of the core vitrectomy, the posterior hyaloid was carefully elevated using the vitreous cutter for patients without posterior vitreous detachment. Dilute indocyanine green was used to aid in visualization of the ILM. In every case, the ILM was peeled in a circumferential pattern from around the edge of the MH. An initial flap of ILM was created based on surgeon's preference, either by direct engagement with vitreoretinal forceps or with a diamond-dusted membrane scraper. The remaining membrane peel was completed with vitreoretinal forceps. After an air–fluid exchange, perfluoropropane gas or sulfur hexafluoride gas was used as tamponade agents. Selection of gas was based on surgeon's preference. Patients were instructed to maintain facedown positioning for 1 week postoperatively.

## Intraoperative OCT Image Protocol and Analysis

The Bioptigen SDOIS system attached to the surgical microscope was used intraoperatively, as previously described.<sup>23,30</sup> Imaging was analyzed at two surgical time points: immediately before initiation of pars plana vitrectomy (preincision scan) and after ILM peeling (postpeel scan). A consistent image acquisition protocol was used, including 10 × 10-mm volume scan at 0° and 90°, 10 × 5-mm volume scans with oversampling for averaging, and 10-mm radial volume scans. Each scan consisted of 100 B-scans distributed across the area with 1000 A-scans per B-scan.

Data obtained from iOCT were exported for computer-aided analysis. OCT scans were initially examined for image quality, and eyes with insufficient image quality for assessment of MH boundaries were excluded from the study as previously described.<sup>30,31</sup> At each surgical time point (i.e., prior to ILM peel and following ILM peel), MH boundary segmenta-

**Table 1.** Patient Baseline Clinical Characteristics

Number of eyes (patients)	37 (37)
Age, years, mean $\pm$ SD	66.0 $\pm$ 8.0
Sex, <i>n</i> (%)	
Male	13 (35%)
Female	24 (65%)
Preoperative BCVA	
LogMAR, mean $\pm$ SD	0.91 $\pm$ 0.46
Snellen equivalent, mean	20/164
Preincision minimal width of MH, <i>n</i> (%)	
$\leq 250$ $\mu\text{m}$	14 (38%)
$>250$ $\mu\text{m}$ but $\leq 400$ $\mu\text{m}$	12 (32%)
$>400$ $\mu\text{m}$	11 (30%)
Lens status	
Phakic, <i>n</i> (%)	30 (81%)
Pseudophakic, <i>n</i> (%)	7 (19%)
Combined cataract surgery, <i>n</i> (%)	30 (81%)

BCVA, best corrected visual acuity; logMAR, logarithm of the minimum angle of resolution; SD, standard deviation.

tion was performed with volumetric (e.g., 3-D) reconstruction. This segmentation allowed for multiple measurements to be completed, including MH volume, height, minimal width, and depth. In addition, manual measurements of the ellipsoid zone (EZ)-retinal pigment epithelium (RPE) height were performed, as previously described.<sup>29</sup>

### Clinical OCT Imaging Outside the Operating Room

OCT images were obtained (Cirrus HD-OCT, model 5000; Carl Zeiss Meditec, Dublin, CA) using the 512  $\times$  128 scan pattern and high-definition five-line raster pattern at each time point. Patients were scanned preoperatively, at 1 day, 2 weeks, 1 month, and 3 months postoperatively. Scans from preoperative and postoperative time points were analyzed for the existence of MH and concurrent macular diseases. Visual acuity was measured at the preoperative examination and all postoperative time points. Significant visual improvement (or decline) was defined as an increase (or decrease) by two or more lines on a Snellen chart. Snellen visual acuity was converted to the logarithm of the minimum angle of resolution (logMAR) scale for analysis.

### Statistical Analyses

For each patient, 19 perioperative clinical variables, including MH status on POD 1, sex, lens status,

age, preincision EZ-RPE height, post-ILM peel EZ-RPE height, post-ILM peel EZ-RPE expansion, preincision volume, preincision height, preincision minimal width, preincision depth, post-ILM peel volume, post-ILM peel height, post-ILM peel minimal width, post-ILM peel depth, change in volume, change in height, change in minimal width, and change in depth were collected (Figs. 1, 2). Results are expressed as a mean  $\pm$  standard deviation. Data analyses were performed using software (R software version 3.2.3; Software Foundation's GNU project, in the public domain, <https://www.r-project.org/>). Univariate analysis was used to evaluate whether clinical variables were associated with the MH closure status. Fisher's exact test was used for two categorical clinical variables (sex and lens status), and two-sample *t*-test was performed for continuous clinical variables. Subsequently, multivariate logistic regression analysis was used to determine statistically significant predictors for MH closure.

## Results

### Clinical Demographics and Characteristics

The baseline clinical demographics and characteristics of the patients are summarized in Table 1. Overall, 62 eyes were identified that underwent surgical repair for MH. Ten eyes were excluded due to lack of trans-gas OCT image, and 15 eyes were excluded for lack of sufficient iOCT data. Hence, 37 eyes from 37 patients were included in the analysis. The mean age of patients was 66.0  $\pm$  8.0 years (range, 50–80). The mean preoperative visual acuity was 20/164, range 20/30 to 20/2000 (e.g., logMAR visual acuity 0.91  $\pm$  0.46). Seven eyes were pseudophakic preoperatively; the remaining 30 eyes received phacoemulsification and IOL implantation at the time of the MH surgery. Preoperative MH minimum width was as follows: 14 (38%) eyes were  $\leq 250$   $\mu\text{m}$ , 12 (32%) eyes were  $>250$   $\mu\text{m}$  but  $\leq 400$   $\mu\text{m}$ , and 11 (30%) eyes were  $>400$   $\mu\text{m}$ .

On POD 1, MH closure was confirmed in 32 (86%) eyes; MH closure rate based on preincision minimal width was 100% (14/14) in eyes with  $\leq 250$   $\mu\text{m}$ , 75% (9/12) in eyes with  $>250$   $\mu\text{m}$  but  $\leq 400$   $\mu\text{m}$ , and 82% (9/11) in eyes with  $>400$   $\mu\text{m}$ . At a 3-month visit, MH closure was achieved in 35 (95%) eyes; MH closure rate based on preincision minimal width was 100% (14/14) in eyes with  $\leq 250$   $\mu\text{m}$ , 92% (11/12) in eyes with  $>250$   $\mu\text{m}$  but  $\leq 400$   $\mu\text{m}$ , and 91% (10/11) in eyes with  $>400$   $\mu\text{m}$ . The reopening of a MH was observed

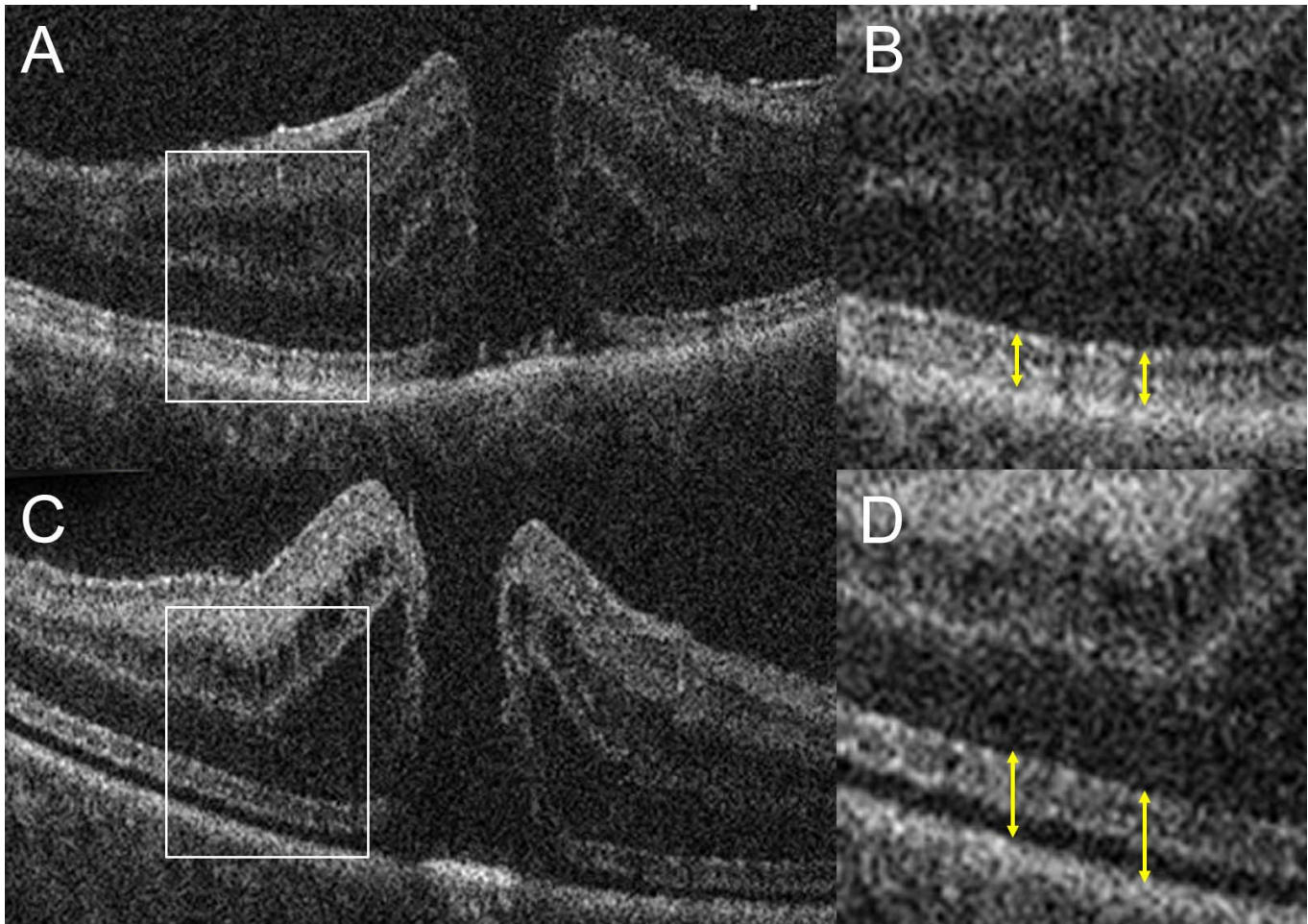


**Figure 1.** A representative case example of MH demonstrating alterations in retinal microstructure on intraoperative OCT before and after ILM peeling. (A, B) In B-scan prior to ILM peeling, highly reflective lines in the outer retina, including EZ, are observed (A). In the magnified view, the distance between EZ to RPE appears within the normal range (*yellow double-sided arrow*) (B). (C, D) After ILM peeling, a slight increase in the MH depth, and diffuse expansion of EZ to RPE height (*yellow double-sided arrow*) indicative of shallow retinal detachment are observed (D).

in one (3%) eye at 3 months postoperatively. Mean postoperative visual acuity was 20/58, range 20/20 to 20/2000 (logMAR visual acuity  $0.46 \pm 0.46$ ). Twenty-nine (78%) eyes had a significant increase in visual acuity, while one (3%) eye with a persistent MH had a decrease in visual acuity.

The summary statistics are listed in [Table 2](#). After univariate analysis, seven variables showed potential significant difference ( $P < 0.20$ ) between patients with persistent MH and patients with closed MH on POD 1: age, post-ILM peel EZ-RPE expansion, preincision minimal width, post-ILM peel depth, change in volume, change in minimum width, and change in depth. Next, these selected seven variables were used to fit a multivariate logistic regression. [Table 3](#) shows the parameter estimation for such a multivariate

logistic regression. The final prediction model is:

$$\begin{aligned} &\text{Probability of POD 1 MH closure (\%)} \\ &= \frac{e^{\eta}}{1 + e^{\eta}} \times 100\% \end{aligned}$$

where:

$$\begin{aligned} \eta = &48.72 - 0.634 \times \text{Age} \\ &+ 1.146 \times 10^{-4} \times \text{post-ILM peel EZ-RPE expansion} \\ &- 2.838 \times 10^{-2} \times \text{Preincision minimal width} \\ &+ 8.753 \times 10^{-3} \times \text{post-ILM peel depth} \\ &- 7.009 \times 10^2 \times \text{Change in volume} \\ &+ 9.499 \times 10^{-2} \times \text{Change in minimum width} \\ &+ 2.512 \times 10^{-2} \times \text{Change in depth.} \end{aligned}$$

Using the selected seven variables, the area under

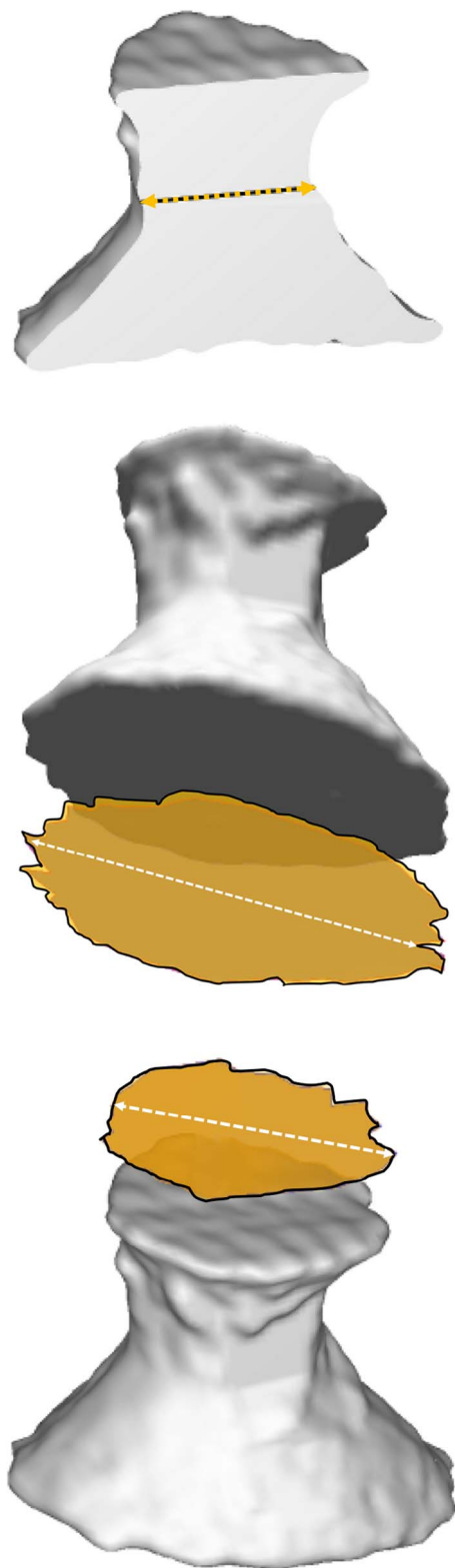


**Figure 2.** Three-dimensional visualization of MH and feasibility of measurement of MH parameters utilizing the MH segmentation platform, including linear dimensions, areas, and volume.

the curve (AUC) is 0.974, suggesting that the model demonstrated an excellent fit to the data. One concern was that the small sample size (37 eyes) may lead to the overfitting issue. To address this issue, we further performed the cross-validation analysis. Specifically, among all 32 patients with closed MH on POD 1, we randomly selected 22 patients into the training set and put the remaining 10 patients into the testing set. In addition, among all five patients with persistent MH on POD 1, we randomly selected three patients into the training set and put the remaining two patients into the testing set. Next, we fitted a multivariate logistic regression with seven variables using the training set, which consisted of 25 patients, and then tested its prediction performance in the testing set, which consisted of 12 patients. We repeated such cross-validation analysis 10 times. Across 10 cross-validation analyses, the AUC achieved a mean 0.82 and standard deviance 0.08, indicating that the multivariate logistic regression does not suffer from the overfitting problem. We further evaluated the parameter estimates in each of 10 cross-validation analysis and found that three variables, including preincision minimal width, change in volume, and change in minimal width, show consistent estimated direction among all 10 cross-validation analyses (Table 4). Therefore, these three variables are highly robust predictors for the MH closure status. The relationship between preincision minimal width, change in volume, and change in minimal width are shown in scatter plot (Fig. 3). The regression line in both scatter plots had a small negative slope, suggesting a weak negative association. After ILM peeling, minimal width showed a tendency to increase in small MHs. Conversely, minimal width showed a tendency to decrease in large MHs.

## Discussion

In this report, we describe, we believe for the first time, a prediction model for MH closure speed based on a panel of iOCT variables. By the identification of preoperative patient characteristics and the quantification analysis of multiple perioperative OCT variables, we were able to discriminate patients with early anatomical outcomes from patients without early closure on POD 1. In our prediction model for MH closure utilizing seven covariates, the area under receiver operator characteristic curve was 0.974, with high sensitivity and high specificity. It is interesting that five out of seven covariates identified as independent predictors for successful MH closure

**Table 2.** Parameter Analysis Summary

Variables	Type	Summary	Association With POD 1 MH Closure, P-Value
POD 1 MH status	Categorical	Closed MH: 32, persistent MH: 5	Primary outcome
Sex	Categorical	Male: 13, Female: 24	0.638 <sup>a</sup>
Lens status	Categorical	Phakic: 30, Pseudophakic: 7	0.560 <sup>a</sup>
Age, y	Continuous	66.0 ± 8.0 (50, 80)	0.077 <sup>*b</sup>
Preincision EZ-RPE height, μm	Continuous	45.3 ± 7.1 (32.0, 66.8)	0.633 <sup>b</sup>
Post-ILM peel EZ-RPE height, μm	Continuous	53.7 ± 8.7 (38.4, 78.5)	0.253 <sup>b</sup>
Post-ILM peel EZ-RPE expansion	Continuous	6085 ± 4805 (1155, 30320)	0.108 <sup>*b</sup>
Preincision volume, mm <sup>3</sup>	Continuous	0.126 ± 0.161 (0.008, 0.902)	0.557 <sup>b</sup>
Preincision height, μm	Continuous	471 ± 118 (204, 773)	0.888 <sup>b</sup>
Preincision minimal width, μm	Continuous	340 ± 234 (15, 960)	0.124 <sup>*b</sup>
Preincision depth, μm	Continuous	851 ± 639 (231, 4206)	0.721 <sup>b</sup>
Post-ILM peel volume, mm <sup>3</sup>	Continuous	0.100 ± 0.117 (0.005, 0.608)	0.344 <sup>b</sup>
Post-ILM peel height, μm	Continuous	465 ± 113 (158, 737)	0.366 <sup>b</sup>
Post-ILM peel minimal width, μm	Continuous	336 ± 193 (70, 790)	0.261 <sup>b</sup>
Post-ILM peel depth, μm	Continuous	697 ± 305 (266, 1431)	0.102 <sup>*b</sup>
Change in volume, mm <sup>3</sup>	Continuous	−0.0258 ± 0.0537 (−0.2944, −0.0280)	0.194 <sup>*b</sup>
Change in height, μm	Continuous	−6.2 ± 51.8 (−179, 90)	0.401 <sup>b</sup>
Change in minimum width, μm	Continuous	−3.9 ± 124.4 (−315, 370)	0.036 <sup>*b</sup>
Change in depth, μm	Continuous	−154 ± 485 (−2785, 405)	0.170 <sup>*b</sup>

Results of continuous variables are expressed as mean ± SD (range from minimum to maximum). \*P-value < 0.20.

<sup>a</sup> Fisher's exact test.

<sup>b</sup> Two-sample t-test.

were iOCT variables that cannot be acquired preoperatively. Many of these variables relate to a “change” in tissue measurements following ILM peeling. This suggests that the change in the tissue may represent a surrogate for tissue elasticity and deformability that may be important variables for how easily the retina reapproximates. In addition, the outer retinal parameters may represent a surrogate for outer retinal/RPE adherence or retinal mobility to allow for more rapid closure. The three most robust predictors were all

iOCT variables, although the preincisional minimum width correlates strongly to preoperative minimum width and might be able to be used instead. The presented data demonstrate that utilizing a panel of iOCT variables may be a promising approach for the individualized care with respect to determining the duration of facedown positioning.

Ever since OCT became available in clinical practice, there have been numerous attempts to utilize the preoperative OCT parameters to predict the

**Table 3.** Parameter Estimation for Multivariate Logistic Regression

Variables	Coefficients	Estimate Standard Error	z-Static	P-Value
(intercept)	4.872 × 10	6.534 × 10	0.746	0.456
Age	−6.340 × 10 <sup>−1</sup>	9.490 × 10 <sup>−1</sup>	−0.668	0.504
Post-ILM peel EZ-RPE expansion	1.146 × 10 <sup>−4</sup>	4.698 × 10 <sup>−4</sup>	0.244	0.807
Preincision minimal width	−2.838 × 10 <sup>−2</sup>	4.405 × 10 <sup>−2</sup>	−0.644	0.519
Post-ILM peel depth	8.753 × 10 <sup>−3</sup>	2.645 × 10 <sup>−2</sup>	0.331	0.741
Change in volume	−7.009 × 10 <sup>2</sup>	9.511 × 10 <sup>2</sup>	−0.737	0.461
Change in minimum width	9.499 × 10 <sup>−2</sup>	1.192 × 10 <sup>−1</sup>	0.797	0.426
Change in depth	2.512 × 10 <sup>−2</sup>	3.433 × 10 <sup>−2</sup>	0.732	0.464

**Table 4.** Parameter Estimation for Multivariate Logistic Regression With Seven Variables, for 10 Cross-Validations

Cross-Validation	Age	Post-ILM Peel EZ-RPE Expansion	Preincision Minimal Width	Post-ILM Peel Depth	Change in Volume	Change in Minimum Width	Change in Depth
1	-8.33	-0.0021	<b>-0.28</b>	-0.02	<b>-10891</b>	<b>1.69</b>	0.57
2	-2.19	0.0063	<b>-0.07</b>	-0.29	<b>-5667</b>	<b>1.44</b>	0.24
3	-4.15	-0.0054	<b>-0.17</b>	0.03	<b>-4109</b>	<b>1.23</b>	0.24
4	-2.15	0.0063	<b>-0.08</b>	-0.29	<b>-5690</b>	<b>1.43</b>	0.24
5	-13.46	0.0081	<b>-0.71</b>	0.26	<b>-7035</b>	<b>0.70</b>	0.10
6	-2.58	0.0086	<b>-0.15</b>	-0.06	<b>-1396</b>	<b>0.29</b>	0.06
7	3.70	-0.0001	<b>-0.66</b>	0.28	<b>-6825</b>	<b>0.06</b>	0.23
8	-0.57	0.0001	<b>-0.03</b>	0.01	<b>-625</b>	<b>0.08</b>	0.02
9	-10.72	0.0131	<b>-0.69</b>	0.29	<b>-3175</b>	<b>0.46</b>	-0.34
10	-5.99	-0.0105	<b>-0.25</b>	0.18	<b>-4712</b>	<b>1.26</b>	0.29

Variables with consistent direction are in bold font.

successful anatomical outcome of MHs. Ip et al.<sup>21</sup> performed preoperative OCT analysis on 40 eyes with MH and reported that smaller MHs (<400 μm) were related to higher hole closure rates. Ullrich et al.<sup>20</sup> also studied 94 patients with MH and reported that both minimum hole diameter and basal hole diameter were negatively correlated with postsurgical closure. Similarly, in another cohort study of 50 eyes, logistic

regression analysis demonstrated that the preoperative basal hole diameter, MH inner opening, and minimum inner diameter were associated with anatomical success.<sup>19</sup> Consistent with those previous studies, we also found that preincision minimal width of MH was a robust predictor. However, we did not find any other predictor associated with preincision OCT variables. It may be reasonable to assume that,

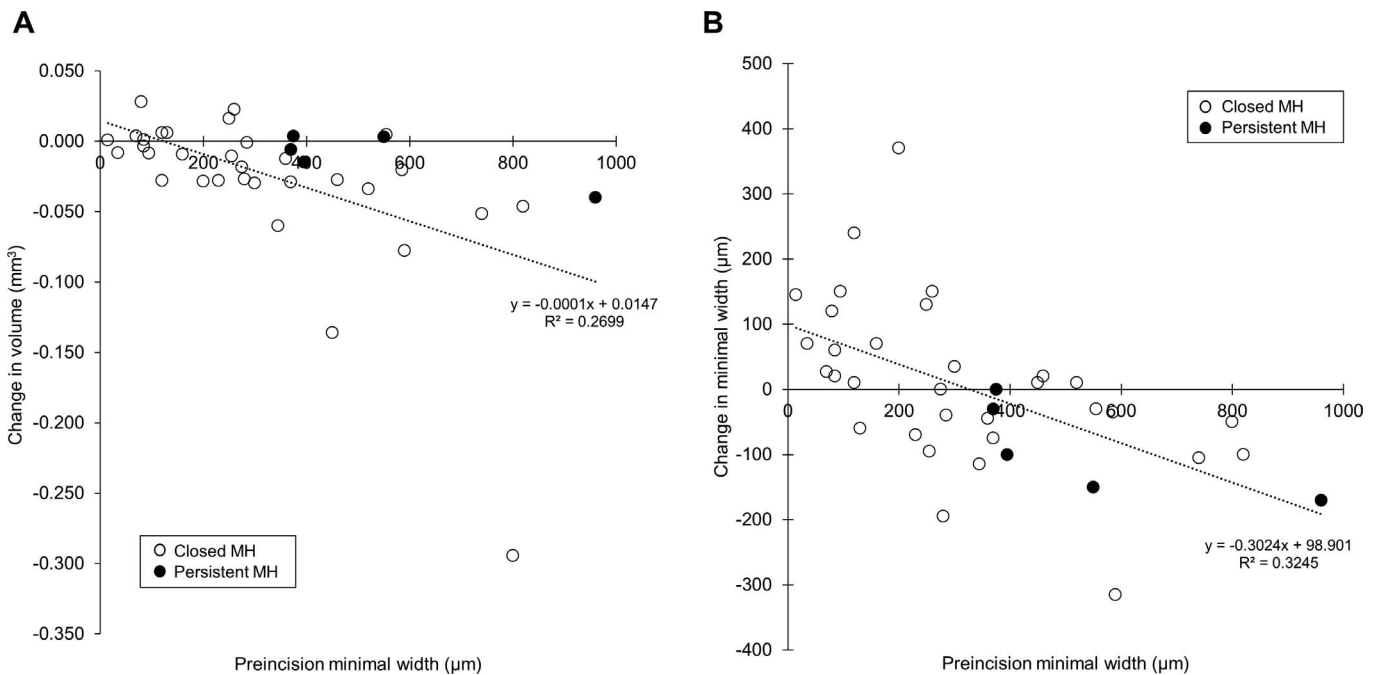


**Figure 3.** Scatter plot with regression line to visualize the relationship between (A) preincision minimal width and change in volume, (B) preincision minimal width and change in minimal width. *Solid* and *open markers* represent each patient with persistent MH and closed MH, respectively.

because the morphology of MHs and ultrastructure of retinal layers change after ILM peeling,<sup>27,30,32</sup> pre-precision OCT variables (except minimal inner diameter) may have less impact on MH closure compared with iOCT variables that can be acquired after ILM peeling given the new information provided by how the tissue responded to the ILM peel.

Other investigators have described a different method to predict MH closure, which was based on postoperative daily OCT examination in gas-filled eyes.<sup>7,15–18</sup> Specifically, patients were allowed to end facedown positioning if the hole was confirmed to be closed on OCT. In this method, the posterior retina was depicted in 80% to 100% of eyes and was able to make moderate to high prediction of persistent MH closure.<sup>7,15–18</sup> One limitation of this protocol is that OCT image cannot be obtained in cases with extensive postvitrectomy debris on the cornea/IOL,<sup>7,18</sup> if the gas bubble is not large enough to cover the posterior pole, and is quite difficult if the patient is phakic.<sup>17</sup> Also, locating the macula correctly can be difficult for some cases when a foveal depression hardly exists immediately after the surgery.<sup>17</sup> In this report, over 15% of eyes were not able to be successfully imaged with trans-gas OCT on POD 1. This highlights some of the challenges for relying solely on a POD 1 trans-gas OCT assessment.

Our prediction model, which depends on multiple iOCT covariates, has several advantages over previous models. Unlike trans-gas OCT analysis, iOCT images can be captured in high probability of imaging success. Also, iOCT may be less subjected to OCT signal attenuation due to cataract, since phacovitrectomy is often performed at the time of the MH repair. Additionally, our prediction model included a change in MH volume, which may be more reliable compared with previously reported models utilizing MH diameter. Given that MHs are not always symmetrical, MH volume with three-dimensional information may reflect better characteristics of MHs compared with MH diameter, which consists only of a single cross-sectional image of a two-dimensional B-scan.<sup>30</sup>

Previously, our group and others have described intraoperative microstructural alterations of MH after surgical manipulations.<sup>27,29,30,32</sup> We recently demonstrated that the change in MH volume and change in minimal width were correlated with postoperative anatomical normalization after univariate analysis,<sup>29,30</sup> and these correlations were maintained in the current study. Our results showed that change in MH volume was negatively correlated with MH closure, indicating that MH volume reduction

was greater in patients with closed MH. After intentional posterior vitreous separation and ILM peeling, both antero-posterior and tangential traction is released; thus, it is clinically logical to assume that MH volume reduction may be associated with successful anatomical outcome. Surprisingly, change in minimal width was positively correlated with MH closure, meaning that minimal width reduction was greater in eyes with persistent MH. This somewhat counterintuitive finding may be explained by the fact that the study comprised various sizes of MH, where small MHs (especially <200  $\mu\text{m}$ ) were likely to increase in minimum width due to surgical trauma of ILM peeling, whereas large MHs (>600  $\mu\text{m}$ ) were likely to decrease in minimum width due to release of tangential traction (Fig. 3B). None of the five eyes with persistent MH had increase in minimal width, whereas 50% (16/32) of eyes with closed MH had increase in minimal width.

We are aware of several limitations to this study. First, our study is limited by small sample size. Second, we did not conduct analysis on postoperative visual acuity because the anatomical outcome is the determining factor of visual improvement, thus we sought prediction of MH closure as being more important. We also did not conduct analysis on the staging of the MH, which may have provided additional information regarding posterior vitreous detachment, because these data were not reliably available. Moreover, the variation in ILM peeling technique between surgeons, which may affect the anatomical outcome of the MH, is not accounted for in our predictive model. Furthermore, we did not include MH patients with high levels of myopia due to imaging challenges in these patients.

In future studies, development of a fully automated calculation software/algorithm for OCT measurement MH geometry is warranted. Surgeons then may be able to predict the likelihood of rapid MH closure, which may also be useful in deciding whether the extent of ILM peeling is sufficient. Based on our findings, facedown position strategy may be individualized, where patients with high probability of MH closure may be alleviated or exempted from posturing without confirmation of macula status on trans-gas OCT. Our study confirms the feasibility of iOCT imaging during MH surgery and provides significant evidence that hole closure in the early postoperative period may be highly predicted utilizing multiple iOCT covariates. A future randomized comparative trial is necessary to validate this model and demonstrate its effectiveness compared to standard of care.



Our team was recently awarded an NIH clinical trial planning grant to develop the protocol for this future randomized trial. In conclusion, this predictive model for hole closure speed based on iOCT variables provides an exciting opportunity for image-based decision-making in postoperative care with future validation and may provide unique insights into the role that iOCT measurements may play as surrogates for tissue elasticity and mobility.

## Acknowledgments

The following outlines the contributions of the authors: design of the study (JPE); conduct of the study (all authors); data collection (JPE, SKS); data management (JPE, MH, AU); data analysis (all authors); data interpretation (all authors); preparation of the manuscript (JPE, MH, AU); review and approval of the manuscript (all authors).

Supported by National Institutes of Health/National Eye Institute K23-EY022947-01A1 (JPE); Ohio Department of Development TECH-13-059 (JPE); Research to Prevent Blindness (Cole Eye Institutional Grant); Unrestricted travel grant from Alcon Novartis Hida Memorial Award 2015 funded by Alcon Japan Ltd. (AU).

Disclosure: **J.P. Ehlers**, Regeneron (F), Genentech (F, C), Thrombogenics (F, C), Alcon (F, C), Zeiss (C), Santen (C), Novartis (F, C), Aerpio (F, C), Allergan (C), Bioptigen/Leica (C, P); **A. Uchida**, None; **S.K. Srivastava**, Allergan (F), Bausch and Lomb (C), Zeiss (C), Leica (C), Santen (C), Bioptigen (P); **M. Hu**, None

## References

1. Kelly NE, Wendel RT. Vitreous surgery for idiopathic macular holes: results of a pilot study. *Arch Ophthalmol*. 1991;109:654–659.
2. Lois N, Burr J, Norrie J, et al. Internal limiting membrane peeling versus no peeling for idiopathic full-thickness macular hole: a pragmatic randomized controlled trial. *Invest Ophthalmol Vis Sci*. 2011;52:1586–1592.
3. Haritoglou C, Reiniger IW, Schaumberger M, Gass CA, Priglinger SG, Kampik A. Five-year follow-up of macular hole surgery with peeling of the internal limiting membrane: update of a prospective study. *Retina*. 2006;26:618–622.
4. Kadonosono K, Itoh N, Uchio E, Nakamura S, Ohno S. Staining of internal limiting membrane in macular hole surgery. *Arch Ophthalmol*. 2000;118:1116–1118.
5. Alberti M, la Cour M. Face-down positioning versus non-supine positioning in macular hole surgery. *Br J Ophthalmol*. 2015;99:236–239.
6. Iezzi R, Kapoor KG. No face-down positioning and broad internal limiting membrane peeling in the surgical repair of idiopathic macular holes. *Ophthalmology*. 2013;120:1998–2003.
7. Yamashita T, Sakamoto T, Sonoda S, et al. Individualized, spectral domain-optical coherence tomography-guided facedown posturing after macular hole surgery: minimizing treatment burden and maximizing outcome. *Retina*. 2014;34:1367–1375.
8. Lange CA, Membrey L, Ahmad N, et al. Pilot randomised controlled trial of face-down positioning following macular hole surgery. *Eye (Lond)*. 2012;26:272–277.
9. Guillaubey A, Malvitte L, Lafontaine PO, et al. Comparison of face-down and seated position after idiopathic macular hole surgery: a randomized clinical trial. *Am J Ophthalmol*. 2008;146:128–134.
10. Nadal J, Delas B, Pinero A. Vitrectomy without face-down posturing for idiopathic macular holes. *Retina*. 2012;32:918–921.
11. Au Eong KG, Beatty S, Thomas W, Sen V, Turner GS. Pulmonary embolism following head positioning for retinal reattachment surgery in a young patient with factor V leiden mutation. *Arch Ophthalmol*. 2000;118:1300–1301.
12. Holekamp NM, Meredith TA, Landers MB, et al. Ulnar neuropathy as a complication of macular hole surgery. *Arch Ophthalmol*. 1999;117:1607–1610.
13. Salam A, Harrington P, Raj A, Babar A. Bilateral ulnar nerve palsies: an unusual complication of posturing after macular hole surgery. *Eye (Lond)*. 2004;18:95–97.
14. Tadayoni R, Vicaut E, Devin F, et al. A randomized controlled trial of alleviated positioning after small macular hole surgery. *Ophthalmology*. 2011;118:150–155.
15. Chow DR, Chaudhary KM. Optical coherence tomography-based positioning regimen for macular hole surgery. *Retina*. 2015;35:899–907.
16. Shah SP, Manjunath V, Rogers AH, Bauman CR, Reichel E, Duker JS. Optical coherence tomog-

- raphy-guided facedown positioning for macular hole surgery. *Retina*. 2013;33:356.
17. Masuyama K, Yamakiri K, Arimura N, Sonoda Y, Doi N, Sakamoto T. Posturing time after macular hole surgery modified by optical coherence tomography images: a pilot study. *Am J Ophthalmol*. 2009;147:481–488, e482.
  18. Eckardt C, Eckert T, Eckardt U, Porkert U, Gesser C. Macular hole surgery with air tamponade and optical coherence tomography-based duration of face-down positioning. *Retina*. 2008;28:1087–1096.
  19. Wakely L, Rahman R, Stephenson J. A comparison of several methods of macular hole measurement using optical coherence tomography, and their value in predicting anatomical and visual outcomes. *Br J Ophthalmol*. 2012;96:1003–1007.
  20. Ullrich S, Haritoglou C, Gass C, Schaumberger M, Ulbig MW, Kampik A. Macular hole size as a prognostic factor in macular hole surgery. *Br J Ophthalmol*. 2002;86:390–393.
  21. Ip MS, Baker BJ, Duker JS, et al. Anatomical outcomes of surgery for idiopathic macular hole as determined by optical coherence tomography. *Arch Ophthalmol*. 2002;120:29–35.
  22. Liu P, Sun Y, Dong C, et al. A new method to predict anatomical outcome after idiopathic macular hole surgery. *Graefes Arch Clin Exp Ophthalmol*. 2016;254:683–688.
  23. Ehlers JP, Dupps WJ, Kaiser PK, et al. The Prospective Intraoperative and Perioperative Ophthalmic ImagiNg with Optical CoherEncE TomogRaphy (PIONEER) Study: 2-year results. *Am J Ophthalmol*. 2014;158:999–1007.
  24. Ehlers JP, Tao YK, Srivastava SK. The value of intraoperative optical coherence tomography imaging in vitreoretinal surgery. *Curr Opin Ophthalmol*. 2014;25:221–227.
  25. Ehlers JP, Goshe J, Dupps WJ, et al. Determination of feasibility and utility of microscope-integrated optical coherence tomography during ophthalmic surgery: the DISCOVER Study RE-SCAN results. *JAMA Ophthalmol*. 2015;133:1124–1132.
  26. Binder S, Falkner-Radler CI, Hauger C, Matz H, Glittenberg C. Feasibility of intrasurgical spectral-domain optical coherence tomography. *Retina*. 2011;31:1332–1336.
  27. Ray R, Baranano DE, Fortun JA, et al. Intraoperative microscope-mounted spectral domain optical coherence tomography for evaluation of retinal anatomy during macular surgery. *Ophthalmology*. 2011;118:2212–2217.
  28. Toygar O, Riemann CD. Intraoperative optical coherence tomography in macula involving rhegmatogenous retinal detachment repair with pars plana vitrectomy and perfluoron. *Eye (Lond)*. 2016;30:23–30.
  29. Ehlers JP, Itoh Y, Xu LT, Kaiser PK, Singh RP, Srivastava SK. Factors associated with persistent subfoveal fluid and complete macular hole closure in the PIONEER study. *Invest Ophthalmol Vis Sci*. 2015;56:1141–1146.
  30. Ehlers JP, Xu D, Kaiser PK, Singh RP, Srivastava SK. Intrasurgical dynamics of macular hole surgery: an assessment of surgery-induced ultrastructural alterations with intraoperative optical coherence tomography. *Retina*. 2014;34:213–221.
  31. Xu D, Yuan A, Kaiser PK, et al. A novel segmentation algorithm for volumetric analysis of macular hole boundaries identified with optical coherence tomography. *Invest Ophthalmol Vis Sci*. 2013;54:163–169.
  32. Dayani PN, Maldonado R, Farsiu S, Toth CA. Intraoperative use of handheld spectral domain optical coherence tomography imaging in macular surgery. *Retina*. 2009;29:1457–1468.